Isı Bilimi ve Tekniği Dergisi, 35, 1, 21-26, 2015
J. of Thermal Science and Technology

ISSN 1300-3615

RESOLVING TURBULENT FLAME FRONT FROM MIE SCATTERING MEASUREMENTS

Bertan KAYNAROĞLU[*] and Onur TUNÇER[**]
[*]Istanbul Technical University, Faculty of Aeronautics and Astronautics, 34469, Istanbul, Turkey,
kaynaroglu@itu.edu.tr
[**]Istanbul Technical University, Faculty of Aeronautics and Astronautics, Maslak, 34469, Istanbul, Turkey,
tuncero@itu.edu.tr

(Geliş Tarihi: 18.11.2013, Kabul Tarihi: 18.03.2014)

Abstract: Turbulent swirl stabilized methane/air flames were studied to investigate the flame front characteristics. Swirl number and equivalence number were selected as 0.74 and 0.7 respectively. This study is mainly based on image processing algorithms. Therefore flame front information is recovered from Mie scattering images. Flame edges were detected by Canny edge detection algorithm. Statistical analysis was applied to instantaneous flame front areas and velocity vectors which were provided from Mie scattering images. In addition, fractal approach was employed to the flame front areas to predict the wrinkling factor thus the turbulent flame speed. As a consequence flame front was stabilized both on the edge of the inner and outer shear layer. Turbulent burning velocity was provided on the flame front by superposition of flame front found from Mie images and velocity data analyzed from Particle Image Velocimetry (PIV). Furthermore, flame area ratios were procured to reason the flame front wrinkling factor and the fractal approach to determine turbulent burning velocity. The probability density function of the turbulent flame speeds and flame area fluctuations appear to be Gaussian in shape. Measurements demonstrate that flame wrinkling increases the burning velocities by almost an order of magnitude.
Keywords: Swirl flows, Combustion, Turbulent flame, Flame front edge detection

MIE SAÇILIMLARI YÖNTEMİ İLE TÜRBÜLANSLI ALEV CEPHESİ ÇÖZÜMLEMESİ

Özet: Girdap ile stabilize edilmiş türbülanslı metan/hava alevleri, alev cephesi karakteristiklerini incelemek için çalışılmıştır. Girdap sayısı ve eşdeğerlilik oranı sırasıyla 0.74 ve 0.7 olarak seçilmiştir. Bu çalışmada daha ziyade görüntü işleme algoritmaları üzerinde durulmuştur. Dolayısıyla alev cephesinin konumu Mie saçılımı görüntüleri yardımıyla tayin edilmiştir. Alevin kollarının konumu Canny kenar bulma algoritması kullanılarak belirlenmiştir.
Anlık alev cephesi konumu ve hız vektörleri kullanılarak alev cephesinin alanındaki değişim istatistiki olarak incelenmiştir. Buna ilaveten, alev cephesi üzerinde fraktal yaklaşım uygulanarak alevin buruşma faktörü ve dolayısıyla türbülasnlı alev ilerleme hızı tahmin edilmiştir. Sonuç olarak, alev cephesi girdap vanesi tarafından yaratılan hem iç hem de dış hız değişim katmanlarının kenarlarında stabilize edilmiştir. Parçacık Görüntüleme ile Hız Tayini (PIV) ölçümlerinden elde edilen Mie saçılımı görüntüleri ve hız verileri incelenmiştir. Türbülanslı alev hızı Mie saçılımı görüntüleri işlenerek bulunan alev cephesi konumunun üzerine hız vektörlerinin süperempoze edilmesi sonucu bulunmuştur. Bunlara ek olarak, alev alanı oranından, alev buruşmasından fraktal yöntemle türbülanslı alev hızları elde edilmiştir. Türbülanslı alev hızlarının ve alev alanı çalkantılarının istatistiki yoğunluk fonksiyonlarının Gauss dağılımı şeklinde olduğu görülmektedir. Ölçümler alev cephesinin buruşmasının yanma hızlarını neredeyse bir mertebe daha arttırdığını ortaya koymaktadır.
Anahtar Kelimeler: Girdaplı akışlar, Yanma, Türbülanslı alev, Alev cephesi kenar belirleme

INTRODUCTION

Swirl stabilized premixed combustion is often used in internal combustion and gas turbine engines, furnaces, gasifiers and boilers to increase the heat and mass transfer. Swirl stabilized combustors have substantial advantages in terms of improved combustion efficiency, better ignition stability, and reduced pollutant emissions. These benefits are believed to be the consequence of increased mixing rates due to enhanced turbulence levels (Huang et al., 2003).

The first explanation of turbulent flame propagation is due to Damköhler (Damköhler, 1940). Damköhler defines two distinct regimes which are called small and large scale turbulence. For small scale turbulence, turbulent eddies modify the transport mechanism within the reaction zone which is named as preheat zone. For large-scale turbulence on the other hand, turbulence and flame interaction is believed to be purely kinematic. These two regimes correspond to thin reaction zone and corrugated flamelet regimes respectively. Turbulent flame speed in the present study is calculated from this

approach regarding that the combustor is working under turbulent conditions.

The interaction between turbulent flow field and the flame front is classified using Borghi-Peters diagram through a number of dimensionless parameters. These are the turbulent Reynolds number (Re_T), Damköhler number (Da), and Karlovitz number (Ka). Reynolds number is the ratio of inertial forces to viscous forces. The region under Re_T=1 line is termed as laminar flames. Damköhler number plays an important role since strong time dependency of turbulent phenomena that is defined as the ratio of the characteristic flow time scale to characteristic chemical reaction time. Combustion process is controlled by chemical kinetics, with decreasing Damköhler number (Da<1) corresponds to the stirred reactor zone while large Damköhler numbers (Da>>1) defines several regimes, which are called flamelet regimes. Furthermore, large Damköhler number refers to fast chemistry, as the chemical time scale is smaller with respect to turbulent flow time scale. Lastly Karlovitz number defines the relation between the laminar flame thickness (δ_L) and the smallest turbulent flow scale epitomized as Kolmogorov microscale (η). Borghi-Peters diagram and corresponding regime boundaries can be seen from Figure 1.

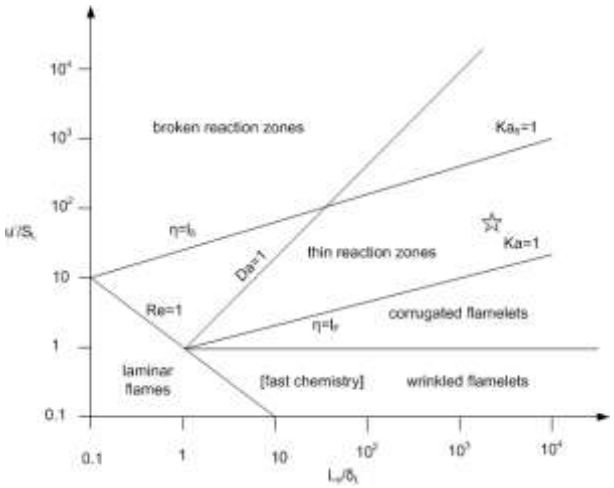

Figure 1. Borghi-Peters diagram (test conditionindicated with a star symbol)

Corrugated and wrinkled flamelet regimes are restricted with Ka=1 line in the Borghi-Peters regime diagram. In these regimes interaction between flame front and the turbulent flow field is purely kinematic (Siewert, 2006). Wrinkled flame regime is similarly confined by the u'/S_L=1 line. Under this line laminar flame speed dominates the turbulent fluctuations. Therefore the thickness of the flame front is not altered by turbulence as the Kolmogorov eddies are so much larger than the laminar flame thickness. In the corrugated flamelet regime, flame front wrinkles more than the wrinkled flamelet regime since turbulent flame speed can be much higher than the laminar flame speed. In this regime "flame pockets" are produced by intense turbulence level nevertheless large Kolmogorov eddies still cannot diffuse into the reaction zone. On the other hand in the thickened flamelet regime, turbulent eddies are small enough to penetrate into the flame front, resulting an increase in heat diffusivity and a corresponding increase in flame thickness (Zimont, 1976).

Another method to obtain the turbulent flame speed is via the fractal approach. Pioneering studies were introduced by Gouldin (1987) and Mandelbrot (1983). Early attempts tried to model the wrinkles with single scale as simple geometric objects. This approach identifies the wrinkles of the flame surface with multiple scales. In the light of the Damköhler's study, the ratio of the turbulent to the laminar flame speed should be proportional to the ratio of the instantaneous flame front area to the mean flame front area (Peters, 1988). Daniele et al. explain their calculation methodologies of fractal parameters, both by the "box counting" (BC) and the "stepping caliper" (SC) methods (Daniele, 2013). Both methodologies are based on the concept of measuring the length of a curve with step size of different scales. Two dimensional fractal dimension D_2 could be found from Eq. 1 by setting, r_i, n_i which correspond to step size and consecutive step of a pre-defined curve. Turbulent burning velocity depends on six parameters, which are average stretched laminar flame speed, instantaneous corrugated flame area, instantaneous inlet flame area, outer and inner cut-off and two fractal dimensions respectively as per Eq. 2. Note that subscript j denotes the index of the instantaneous image. Recent studies can be examined from (Cintosun et al., 2007) and (Wang et al., 2013).

$$n_i \quad \mu \quad r_i^{-D_2} \tag{1}$$

$$S_T = f(S_{L,k}, A_{in,j}, A_{0,j}, e_0, e_1, D_2) \tag{2}$$

An edge detection algorithm is adopted in order to find the turbulence flame speed from the Mie scattering images. Edge detection methods are separated under two categories by Maini and Aggarwal, as gradient based and Laplacian based edge detection respectively (2009). While gradient based algorithms utilize the first derivative of the image in order to find the extremes, on the other hand, Laplacian based algorithms use the second derivative information to find the zero crossings. As a gradient based method, Canny edge detection algorithm was chosen due to its superior edge detection performance in the case of noisy images at the cost of computational complexity. Canny improved some of the existing algorithms by reducing the error rate, good localization and having only one response to a single edge. Comparison with other edge detection algorithms may be found in (Maini and Aggarwal, 2009) and details pertaining to the mathematical method can be examined in (Canny, 1986).

EXPERIMENTAL SETUP

An atmospheric conventional swirl stabilized combustion test rig was built in order to study flame surface area fluctuations to establish combustion knowledge infrastructure for the purpose of gas turbines. The swirl vane has eight blades that are inclined 45° with respect to

the oncoming reactant flow. Swirl number is calculated to be 0.75 with this configuration. Top view of the swirl vane and the center body flame holder are provided in Figure 2. More detail about the swirl vane could be found in (Tunçer et al., 2012). Overall view of the test rig can be seen in Figure 3.

Flow above the dump plane is inspected by the Particle Image Velocimetry (PIV) technique. For visualization, a double cavity Nd:YAG laser operating at 532 nm wavelength is used as the light source. Sheet optics turn the laser line into a thin plane of approximately two millimeters in thickness. The imaging region is located above the dump plane. To record the Mie scattering images a CCD camera with 1600x1200 pixel resolution is used. An optical interference filter centered at 532 nm wavelength with a bandwidth of 10 nm FWHM is used to restrain the natural emission of the flame in order to improve the signal to noise ratio. While calibrating the camera a target marked with a checkerboard pattern is placed parallel to the light sheet and pixel-wise resolution in either direction is adjusted. The illuminated flow area is approximately 150 mm x 240 mm in size.

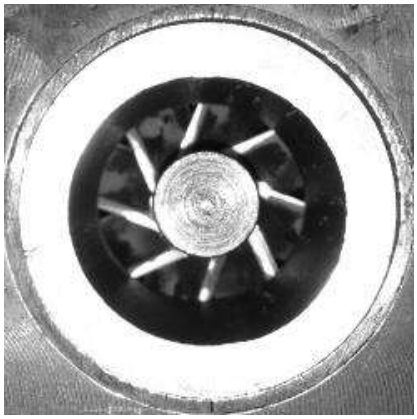

Figure 2. Top view of the swirl vane

Figure 3. Experimental test rig

TiO_2 particles were chosen to seed the flow due to their high temperature resistance and being small enough to follow the fluid. Before each experiment, high humidity inside the seeder drum is removed by simple heaters in order not to allow agglomeration within the test rig. This agglomeration would cause extensive glowing area that yields nearby pixels to loose their brightness relative to this area and consequently bad vectors appear in the calculations.

DATA PROCESSING

At the test condition 276 image pairs were acquired with an inter-pulse time interval $\Delta t=30\mu s$ between images. A 16x16 pixel interrogation window with %75 overlap was used which produces velocity vectors on every fourth pixel, corresponding to a spatial resolution of 2.52 mm in either direction. Average correlation method was chosen since it is a convenient method when the seed particle density changes dramatically within the flow field (Tunçer et al., 2014). Average correlation method correlates each interrogation window one by one at the same point and sums up all the peaks adopted from these interrogation windows to find a velocity vector corresponding to this interrogation area. This operation is iterated for every window. Schematic depiction of the data reduction method is provided in Figure 4.

Mie scattering images are processed to recover the flame front location separating the reactant and the products. At first, Mie images were summed up to find the average scattering image and histogram of this average image was plotted to enhance image properties by both thresholding the gray image and also by adding Gaussian blur etc. Note that while fine smoothing suppresses the noise, excessive smoothing on the other hand destroys the image structure (Ziou and Tabbone, 1988). To focus on the expected flame edges area, a binary mask with ones and zeros was applied to the image where ones correspond to inside of the area. After these steps, the average Mie image was ready for edge detection. Prewitt and Canny methods were tested to determine the edges; nevertheless Canny algorithm yields better results at all.

Canny edge detection algorithm consists of four steps. First the image is convolved with Gaussian blur to eliminate the noise. Gaussian smoothing is then applied by selecting σ value to be 8 pixels within the Canny edge detection algorithm. Gaussian smoothing convoluted the image with a matrix defined by σ value as 8x8. Right after the derivatives on both mutually perpendicular directions were calculated to find the gradient magnitude from the smoothed image. Also the direction of the gradient magnitude was found from the angle between gradient vectors. After that, non-maximum suppression was taken in account to determine whether the pixel had constituted a local maximum on the edge direction. The last step is the hysteresis operator, which explains the threshold value. Any pixel value higher than the lower

threshold level is assumed to be an edge pixel, and if there is a connected edge pixel that is greater than the higher threshold level, it is granted that there is an edge at that pixel. There occurs an edge if the gradient vector remains in between the threshold levels. Detailed procedure can be found in (Ziou and Tabbone, 1988).

Table 1. Data Reduction Scheme with Average Correlation Method

Image No.	Image A		Image B		Correlation	Peak Search and Vector
1	A_1	*	B_1	=	R_{A1B1} +	
2	A_2	*	B_2	=	R_{A2B2} +	
3	A_3	*	B_3	=	R_{A3B3}	
…	…		…		…	
N	A_N		B_N		+	
	Average Correlation				$<R_{AB}>$	Mean Vector →

(a) Frame-I

(b) Frame-II

Figure 4. Color inverted instantaneous Mie scattering images (Re_{Dh}=19400, Sw=0.74, ϕ=0.7, Δt=30μs)

Brighter images were chosen from the paired Mie scattering series to calculate the flame front area over the inner boundary layer created by center body flame holder since the images with sharp brightness and contrast contributes better results with gradient-based edge detection algorithms like "Canny". Inverted Mie images are provided in Figure 4. 95 images from the image set having better brightness and linear or close to linear flame front edges were chosen and flame front area was calculated for each image. The calculated individual flame front areas were non-dimensionalized by the mean flame front area, and histogram was plotted in Figure 8. By Canny edge detection algorithm, flame front, which was observed as a set of points, were combined on a representative line and this procedure has created a linear flame front. Flame area can be calculated from the surface area of a cut cone by the axial-symmetry feature of the flow.

RESULTS AND DISCUSSION

By the nature of swirling flows, flame can be stabilized on three locations; outer shear layer (OSL), inner shear layer (ISL) and vortex breakdown bubble (VBB) (Zhang et al., 2011). In the present case flame stabilizes both at inner and outer shear layers as in Figure 5. When the flow reaches to the dump plane, it expands due to low pressure. A re-circulation zone is established over the center body flame holder which is called as the main re-circulation zone and at the edges of the dump plane there are secondary re-circulation zones that are much weaker than the main re-circulation zone. As one can readily observe the main re-circulation zone from the ISL, mixes the fresh reactants with intermediate combustion products, while inner flame front preheats the mixture steadily. Defined mask in the data processing section was further narrowed down to the inner shear layer (ISL) to allow an observation of the inner vortex properties. Inner shear layer stabilized flame front can be seen from Figure 6.

Figure 5. Visible flame luminosity for the test case, Re_{Dh}=19400, Sw=0.74, ϕ=0.7, (Tunçer et al., 2014)

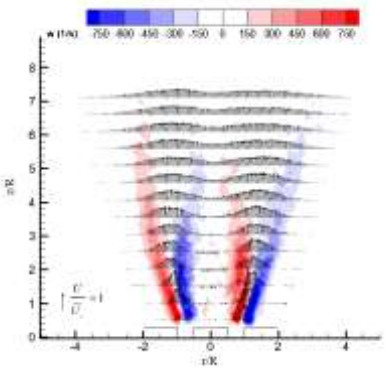

Figure 6. Flame front created by inner shear layer over dump plane, mean velocity profiles and vorticity, Re_{Dh}=19400, Sw=0.74, ϕ=0.7, (non-dimensionalized with respect to the mean axial velocity)

As can be seen from Figure 7, instantaneous flame front areas are closer to averaged flame front areas around a standard deviation, though increasing scattering distribution around the average shows that the flame front is wrinkling to enhance the combustion by turbulence. Lipatnikov and Chomiak (2002) and Lipatnikov (2012) state that flame front wrinkles based on turbulence eddies. While large scale eddies increase the mean flame brush thickness, small scale eddies increase the wrinkles of the flame, which is responsible of increasing turbulent flame velocities.

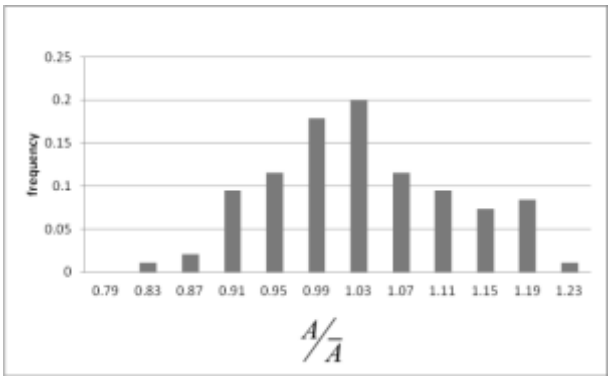

Figure 7. Histogram of the instantenious flame front area non-dimensionalized with respect to the time average value

As a consequence of Damköhler's study (1940), having a turbulent flow condition instead of his Bunsen burner gives us directly the turbulent flame speed from the Mie scattering images that are provided in Figure 8. The turbulent flame front was expected to propagate with that burning velocity relative to the flow field. Note that turbulent flame speed was non-dimensionalized by the laminar flame speed. Laminar flame speed is calculated from the GRI 3.0 mechanism (Smith et al., 1999), it is found to be 0.4 m/s using CANTERA software (Goodwin, 2001). Figure 9 shows the frequency distribution of dimensionless (with respect to the laminar flame speed) turbulent burning velocities. Results indicate on the average three to four fold increase in the flame speed versus the laminar one. The probability density function appears to have a Gaussian shape.

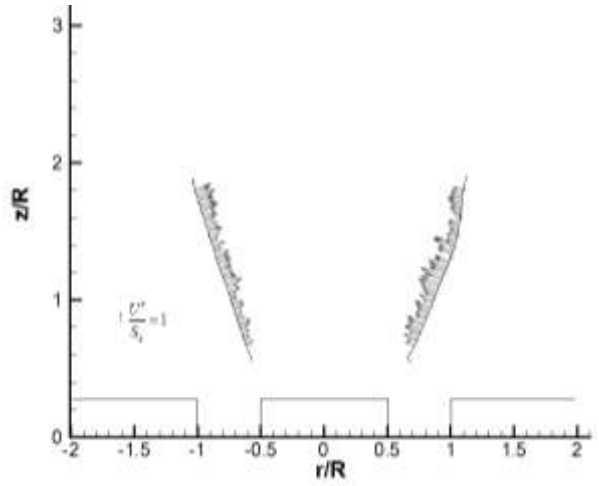

Figure 8. Turbulent burning velocity, Re_{Dh}=19400, Sw=0.74, ϕ=0.7, (non-dimensionalized by laminar flame velocity)

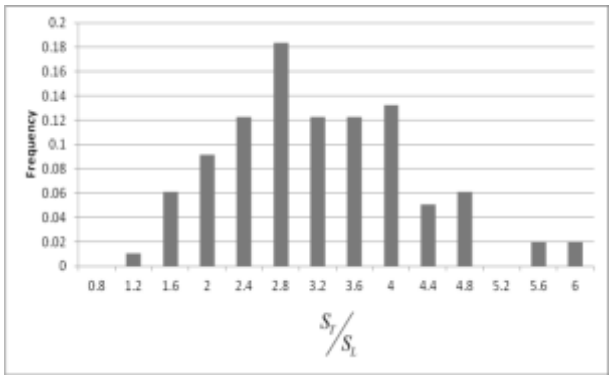

Figure 9. Histogram of the turbulent flame velocities

CONCLUSION

An atmospheric combustion test rig was mainly utilized in order to study flame surface characteristics and turbulent velocity. A wedge shaped flame stabilizes on the edge of the both inner and outer re-circulation zones.

Flame fronts were determined by Canny edge detection algorithm using Mie scattering images. Due to centripetal force and sudden acceleration at the flame front, seed density changes and causing low signal to noise ratios thus edge detection becomes a challenging issue. This was addressed by appropriate image processing methods (i.e. average correlation). Turbulent flame speed measurements agree with predictions. Turbulent flame speeds vary between 2 m/s and 5 m/s. Increasing wrinkling factor in turn increases the flame area and thus the flame speed. This overall process increases the rate of fuel consumption directly and volumetric heat release of the combustor is enhanced.

Results also outline Mie scattering technique as a simple and low cost alternative (with respect to PLIF techniques) for flame front detection. Spatial resolution of flame speed measurements are limited however by the resolution of PIV measurements.

Prospective studies shall focus on determining the fractal parameters in order to prove that the turbulent burning velocity can directly be provided from the velocity data acquired by the particle image velocimetry method.

ACKNOWLEDGEMENT

The authors gratefully acknowledge the financial support received from the Turkish Scientific and Technical Research Council (TÜBİTAK) under contract number 109M426.

REFERENCES

Canny, J., "A computational approach to edge detection. *Pattern Analysis and Machine Intelligence", IEEE Transactions on*, 6, 679-698, 1986.

Cintosun, E., Smallwood, G. J., Gülder, Ö. L., "Flame surface fractal characteristics in premixed turbulent

combustion at high turbulence intensities." *AIAA Journal*, 45(11), 2785-2789, 2007.

Damköhler, G., "Der Einfluss der Turbulenz auf die Flammengeschwindigkeit in Gasgemischen", *Z. Elektrochem*, 46, 601-652, 1940.

Daniele S., Mantzaras J., Jansohn P., Denisov A., Boulouchos K., "Flame front/turbulence interaction for syngas fuels in the thin reaction zones regime: turbulent and stretched laminar flame speeds at elevated pressures and temperatures", *Journal of Fluid Mechanics*, 724, 36-68, 2013.

Goodwin, D.G., Cantera, http://www.cantera.org, 2001-2005.

Gouldin, F.C., "An Application of Fractals to Modelling Premixed Turbulent Flames", *Combustion and Flame*, 68, 249-266, 1987.

Huang Y., Sung H., Hsieh S., Yang V., "Large eddy simulation of combustion dynamics of lean premixed swirl stabilized combustor", *Journal of Power and Propulsion*, 19, 782–794, 2003.

Lipatnikov, A.N., "Fundamentals of Premixed Turbulent Combustion", CRC Press, London, 584 pp., London, 2012.

Lipatnikov, A.N., Chomiak, J., "Turbulent Flame Speed and thickness: phenomenology, evaluation and application in multi-dimensional simulations", *Progress in Energy and Combustion Science*, 28, 1-74, 2002.

Mandelbrot, B.B., *The Fractal Geometry of Nature*, New York: Freeman, 1983.

Maini, R., Aggarwal, H., "Study and comparison of various image edge detection techniques", *International Journal of Image Processing, 3*(1), 1-11, 2009.

Peters, N., "Laminar flamelet concepts in turbulent combustion", *In Symposium (International) on Combustion*, 21:1, 1231-1250. Elsevier, 1988.

Siewert, P., "Flame front characteristics of turbulent lean premixed methane/air flames at high-pressure", Doctoral dissertation, Diss. ETH: 16369, Zurich, 2006.

Smith, G.P., Golden, D.M., Frenklach, M., Moriarty, N.W., Eiteneer, B., Goldenberg, M., Bowman, C. T., Hanson, R.K., Song, S., Gardiner, W.C., Lissianski, Jr.V.V.,Qin, Z.,
http://www.me.berkeley.edu/gri_mech/

Tunçer O., Kaynaroğlu B., Karakaya M. C., Kahraman S., Çetiner-Yıldırım O., Baytaş C., "Preliminary Investigation of a Swirl Stabilized Premixed Combustor", *Fuel*, 115, 870-874, 2014.

Wang, J., Matsuno, F., Okuyama, M., Ogami, Y., Kobayashi, H., Huang, Z., "Flame front characteristics of turbulent premixed flames diluted with CO_2 and H_2O at high pressure and high temperature", *Proceedings of the Combustion Institute*,*34*(1),1429-1436, 2012.

Zhang, Q., Shanbhogue, S. J., Shreekrishna, Lieuwen, T., O'Connor, J., "Strain Characteristics Near The Flame Attachment Point in a Swirling Flow", *Combust. Sci. and Tech*., 183, 665–685, 2011.

Zimont, V., "Theory of turbulent combustion of homogenous fuel mixture at high Reynolds numbers", *Fizika Gorenyia i Vzryva*, 15, 23-32, 1979.

Ziou, D., Tabbone, S, "Edge detection techniques-an overview", *Pattern Recognition and Image Anaylsis C/C of Raspoznavaniye Obrazov I Analiz Izobrazhenii*, *8*, 537-559, 1998.

BERTAN KAYNAROĞLU was born in 1989 in Istanbul, Turkey. Completed high school in 2007 at Üsküdar Çağrıbey (İstanbul). After four years education in Istanbul Technical University he obtained his BSc degree in Astronautical Engineering. He is currently pursuing a MSc.degree in Defense Technologies/Energy Department. He was a research assistant in ITU Combustion Laboratory between 2011-2013. Currently he is a part-time engineer at TUSAŞ Engine Industries. His main research interests are gas turbine engines, combustion, experimental combustion and aerodynamics.

ONUR TUNÇER was born in İzmir in 1979. He graduated from İzmir Science Branch High School in 1997. In 2001 he recevied his BS degree in mechanical engineering from Middle East Technical University. He obtained his PhD degree in the same field from Louisiana State University in 2006. Currently he is an Associate Professor at Istanbul Technical University Department of Aeronautical Engineering.